In-depth Feature Selection for PHM System’s Feasibility Study for Helicopters’ Main and Tail Rotor Actuators

In-depth Feature Selection for PHM System's Feasibility Study for Helicopters' Main and Tail Rotor Actuators

Andrea De Martin[1], Giovanni Jacazio[2], Andrea Nesci[3] and Massimo Sorli[4]

[1,2,3,4] *Politecnico di Torino, Torino, 10129, Italy*
andrea.demartin@polito.it
giovanni.jacazio@formerfaculty.polito.it
andrea.nesci@polito.it
massimo.sorli@polito.it

ABSTRACT

As deeply complex machines subjected to heavy vibratory environment, helicopters require relative low mean time between overhaul and suffer from high maintenance cost and availability issues. So far, PHM for helicopters has been aimed at detecting the presence of structural defects in the most critical parts of the mechanical transmission conveying power from the engine to the rotor blades, but very little has been presented on other flight-critical components, such as the main and tail rotor actuators. The proposed paper is focused on preliminary diagnostics and prognostics considerations for a traditional configuration of hydraulic solution, where a tandem actuator is aided by a Stability and Command Augmentation System (SCAS) during operations.
At first, the case-study is introduced and the simulation model employed for the analysis is described. Hence, two different failure modes affecting the SCAS are investigated and the physical models used to describe their progression are presented. In-depth data mining is then applied to achieve an accurate feature selection from raw data and an original way to visualize features' performances through an accuracy-sensitivity plane is proposed. Lastly, a particle filtering approach is adopted for failure prognosis and its output evaluated through traditional PHM metrics to assess the algorithm effectiveness. The present research provides encouraging results regarding the opportunity of realising a PHM system for helicopters' flight control actuators without the need of additional sensors, which could make solutions based upon the presented work feasible for both in-service and future platforms.

1. INTRODUCTION

Over the years, PHM studies for helicopters have been focused on power supplies and particularly on vibration-based detection techniques for gearbox and drivetrain component (Samuel & Pines, 2005). Despite Main and Tail Rotor Actuators (MRA and TRA) are critical components, PHM has found very limited applications. And although some commonalities can be found with PHM studies for aircraft's hydraulic actuation technologies, even then the most important prognostics system has been developed for electromechanical actuators (Elattar, Elminir, & Riad, 2016) while a lack of references exists on the electro-hydraulic field.
Therefore, Fig. 1 describes one of the possible architecture for the hydraulic actuation with mechanical feedback and Stability and Command Augmentation Systems (SCAS): the present paper aims to a feasibility study of such system. The major difficulty was attributed to a lack of relevant data, because in such a system avionics makes available only few signals:

- SCAS' Electro-Hydraulic Servo Valve (EHSV) current;
- SCAS' actuator displacement;
- MRA/TRA displacement.

Moreover, it has been observed that MRA/TRA displacement was a useless signal since the research has been focused on SCAS' fault modes which have a negligible effect on this signal. Nevertheless, the existing sensors are proved to be sufficient to carry out the prognostics analysis.
Hence, after a brief introduction to the system's physical model and in-depth feature selection is carried out and various evaluation methods are applied. Then the PHM framework, based on an enhanced particle filter, is presented. In the end prognostics results are presented and performances investigated through traditional metrics.

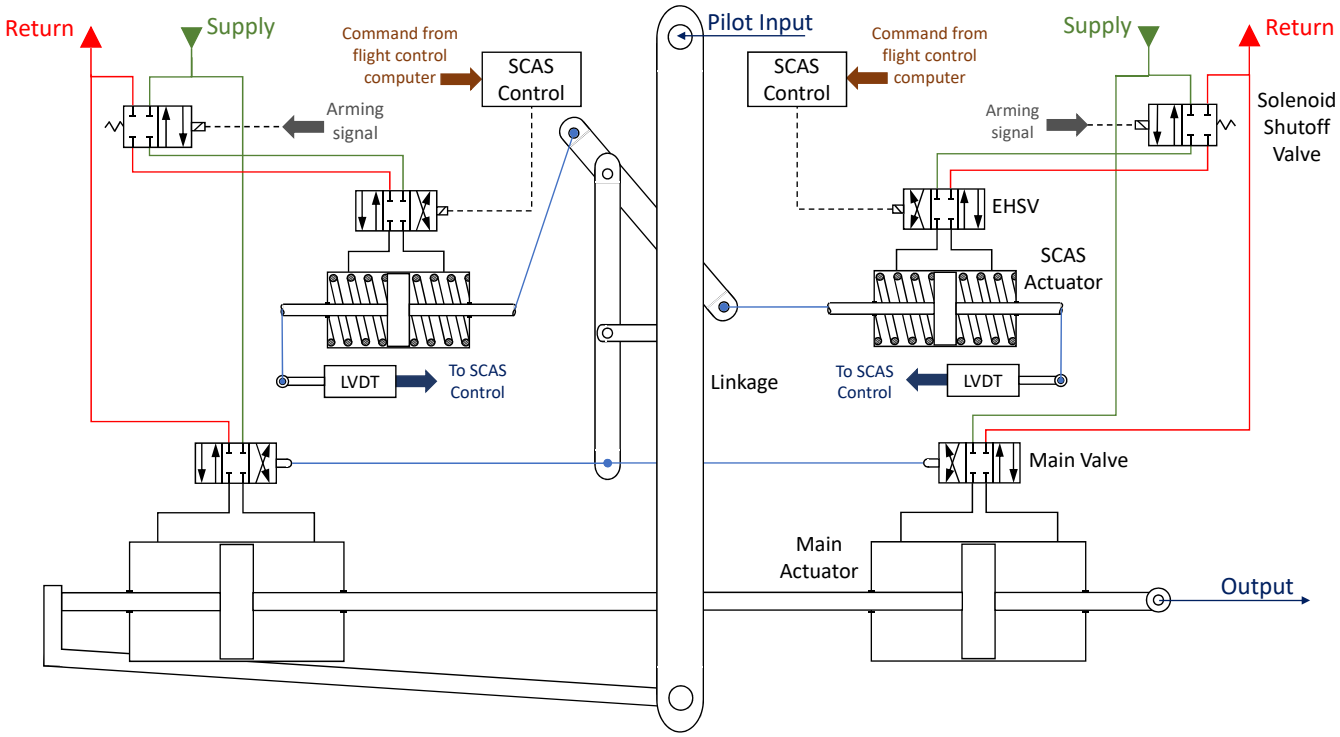

Figure 1. MRA/TRA hydraulic scheme.

2. PHYSICAL MODEL

An high fidelity physical model of the MRA in healthy conditions has been derived and experimentally validated by authors in (De Martin, Dellacasa, Jacazio, & Sorli, 2018). In such healthy system, the degradation models of two significant fault modes of SCAS' actuator have been defined and implemented. In particular, crack propagation in one of the two centering springs and wearing of the actuator piston seals, as depicted in Fig. 2.

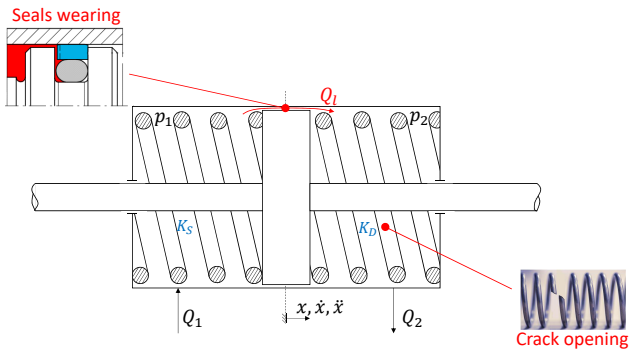

Figure 2. SCAS' actuator fault cases.

2.1. Spring Cracking

The presence of a crack affects the spring stiffness by reducing the resistant area and changing the polar second moment of inertia of the coil's section. An explicit relationship between these two quantities has been obtained by authors in (Nesci, De Martin, Jacazio, & Sorli, 2020). Therefore, crack growth has been estimated by Paris' law (Paris & Erdogan, 1963) while cycle counting has been computed through Rainflow method.

2.2. Seals Wearing

Wearing of the actuator piston seals has been modelled according to Archard's law (Archard, 1953) as accurately elucidated in (Bertolino, Gentile, Jacazio, Marino, & Sorli, 2018). This fault modes implies the increasing of internal leakages in SCAS' actuator, Q_l (please see Fig. 2). At constant pressure difference between the two actuator's chambers, a quadratic relationship has been found between internal leakages and the work of friction forces, L_a, as shown in Fig. 3.
The work of friction forces is easily numerical computable since friction forces and relative displacement between piston and barrel are evaluated during simulations. The Frequency Responce Function (FRF) of the system is strongly affected by internal leakages and particularly the cut-off frequency is inversely proportional to the fault progression as shown by authors in (Nesci et al., 2020). Therefore, failure condition

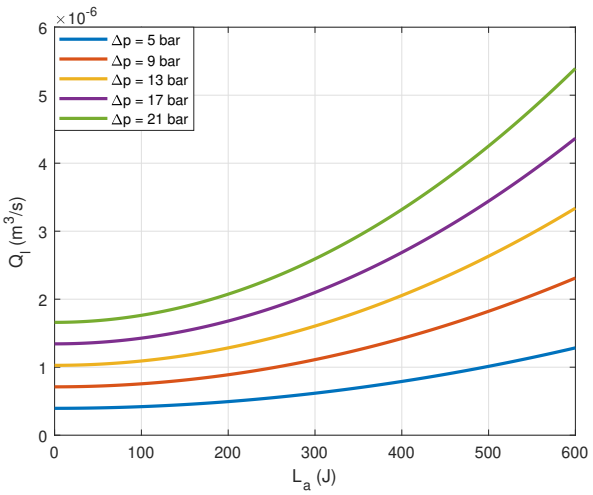

Figure 3. Internal flow rate leakages progression.

has been defined as the time at which the cutoff frequency is 10% lower with respect to the healthy condition one.

2.3. Operational Scenario

Due to the helicopters' unique operating characteristics they're employed in the most varied tasks. Moreover, SCAS' authority is generally limited and its command is mainly dependent on the operational scenario since it derives from an attitude control system. Therefore, SCAS and pilot commands have been randomly accomplished from a set of sinusoidal signals with different amplitudes and frequencies.
Additionally to the in-flight missions, also a pre-flight routine has been developed based on the command sequence for on-ground tests described in (Autin et al., 2018).
Besides the commands, the mission uncertainties concern many other physical parameters and thus such variability sources (i.e. geometrical tolerances, hydraulic fluid properties, external temperature, electrical noise, etc.) have been injected in the model.

3. Data Preparation and Feature Selection

The feature selection process is the linchpin of a good PHM system. It's composed of two different off-line steps (Grosso, De Martin, Jacazio, & Sorli, 2018) first, a trustworthy feature extraction procedure must be defined and for this a physical based approach has been adopted. After that some features have been identified, the best of them are selected to be part of a feature vector, or rather, a sufficient statistic for the system's fault condition (Vachtsevanos, Lewis, Roemer, Hess, & Wu, 2007).

3.1. Feature Candidates

Comparing simulations results between baseline and severe faults conditions, as shown in Fig. 4, the following considerations can be deduced.

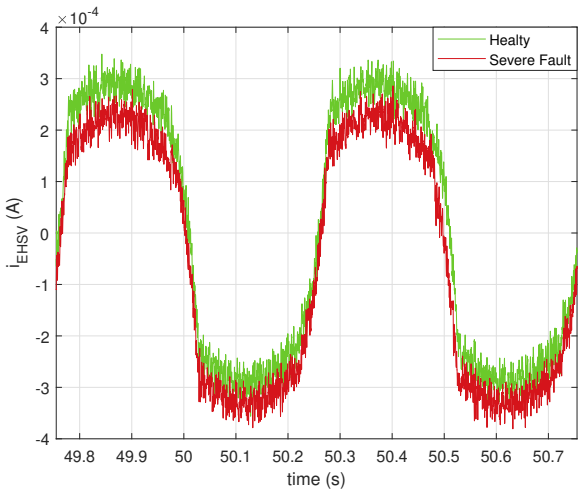

(a) Spring cracking.

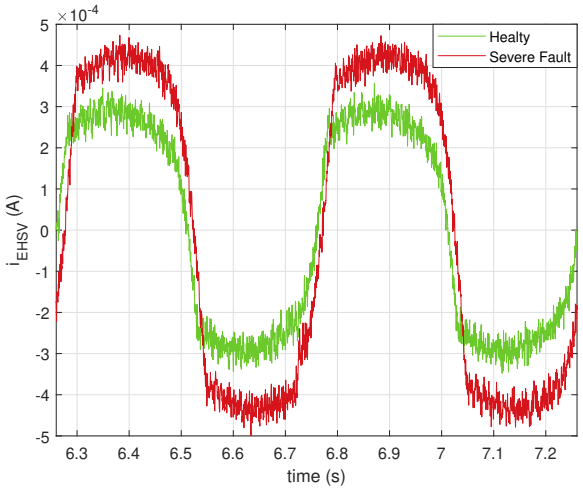

(b) Seal wear.

Figure 4. Servovalve current in baseline and severe fault conditions.

- Spring cracking: as shown previously the stiffness is inversely proportional to the crack size. The asymmetry between the two centering springs' stiffnesses, when one of them is faulty, cause an offset in the resistant force. Therefore, the servovalve current exhibits a null-bias, as depicted in Fig. 4a.
- Seals wear: the leakages originate from seals wear are source of energy loss, so that a greater servovalve current's amplitude is necessary to get the same displacement (Fig. 4b). It results in a reduction of the current-displacement gain between servovalve and SCAS actuator.

The considerations on the physics behind the two faults conducted to the feature candidates contained in Table 1 both for

Table 1. Feature Candidates.

Abbr.	Feature	Description (signal)
$I1$	$abs(fft(x))(2Hz)$	*FFT* amplitude at $2Hz$ (displacement)
$I2$	$mean(xcorr(i, i_h))$	Mean value cross-correlation between actual value and baseline (current)
$I3$	$mean(xcorr(x, x_h))$	Mean value cross-correlation between actual value and baseline (displacement)
$I4$	$mean(xcorr(x))$	Auto-correlation (displacement)
$I5$	$rms(abs(fft(x)))$	*RMS FFT* amplitude (displacement)
$I6$	$rms(x)$	*RMS* (displacement)
$I7$	$rms(i)/rms(x)$	*RMS* gain *EHSV/SCAS*
$G1$	$mean(i)$	Mean value (current)
$G2$	$(max(x) - set)/set$	Overshoot (displacement)
$G3$	i/x	Gain *EHSV/SCAS*

on-ground and in-flight tests.
A first visualization of the features' behaviour is appreciable in Fig. 5: Fig. 5a depicts the probability mass function at three different severities, the farther are the distribution the easier the feature distinguishes the fault mode. Fig. 5b shows the feature's progression with respect to the severity, fluctuations are due to the feature's stochastic nature.

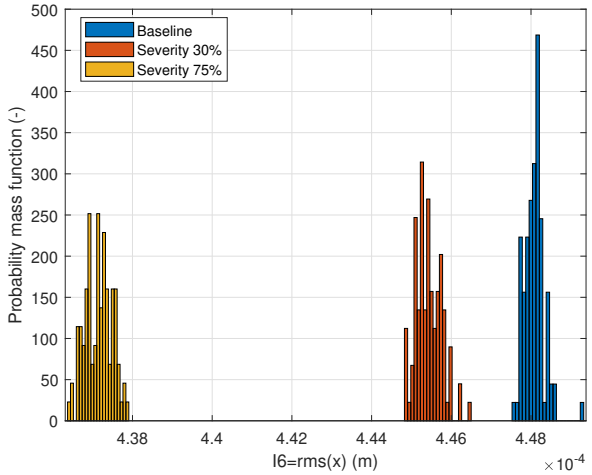

(a) Distribution at three severity.

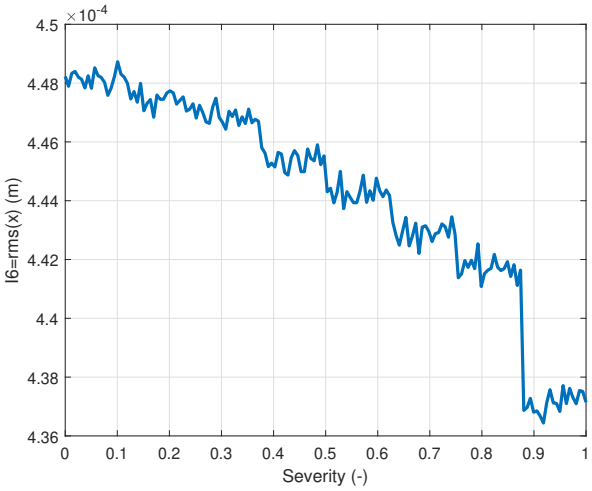

(b) Feature's progression.

Figure 5. Seal wearing I6.

3.2. Feature Selection

The feature selection process aims to extract the most significant subset of features from the original set of collected features (Adams et al., 2017). It doesn't exist an univocal approach to select an optimal subset, moreover, the best features are relative to a certain evaluation criteria (Dash & Liu, 1997). Therefore, various evaluation functions have been computed and the information matched. The process combines three filter methods (Blum & Langley, 1997) and two fault detection's performance metrics.

3.2.1. Redundancies

A divergence measure has been adopted in order to quantify the differences between two different features. That is the Kulloback-Leibler divergence, (Kullback & Leibler, 1951) which is defined, in the discrete case, as follows:

$$D_{KL}\left(P||Q\right) = \sum_{x} P\left(x\right) \log \frac{P\left(x\right)}{Q\left(x\right)} \tag{1}$$

Where $P\left(x\right)$ and $Q\left(x\right)$ are two probability mass function. Eq.(1) satisfies the Gibbs' inequality (Mackay, 2005):

$$D_{KL}\left(P||Q\right) \geq 0 \tag{2}$$

Equality is true if and only if $P = Q$. It has been obtained that:

$$D_{KL}\left(I5||I6\right) \equiv 0 \tag{3}$$

Eq.(3) proves that $I5$ and $I6$ are the same feature, agree with Parseval's identity. Because of the more computational simplicity $I6$ has been preserved and $I5$ discharged.

3.2.2. Correlation Matrix

The first considered ranking property is the Pearson's correlation, a dependence measure that assesses the relationship between the features and both faults (Macky & Roussas, 1999):

$$\rho_{DF} = \frac{\mathbb{E}\left[\left(D - \mu_D\right)\left(F - \mu_F\right)\right]}{\sigma_D\, \sigma_F} \tag{4}$$

Table 2. Correlation by fault and mean SNR of all the features.

Feature	Correlation		SNR (dB)
	Spring	Seal	
$I1$	0.335	-0.110	24.6
$I2$	-0.985	0.250	5.7
$I3$	0.952	-0.958	37.6
$I4$	0.961	-0.949	31.5
$I6$	0.636	0.989	49.9
$I7$	0.017	-0.996	48.5
$G1$	-0.492	0.915	21.4
$G2$	0.783	-0.925	32.3
$G3$	-0.575	0.990	36.7

Where D and F are two random variables (i.e. fault and feature respectively). The results are contained in Table 2.

3.2.3. Signal to Noise Ratio

As the Pearson's correlation defines the relationship between the features and the internal state, the signal to noise ratio measures the feature's sensitivity to the external disturbances. A suitable definition is:

$$SNR = \frac{\mu_F^2}{\sigma_F^2} \tag{5}$$

Results are reported in Table 2.

3.2.4. Performance metrics

A good ranking criteria can be based on feature's performances (Mucciardi & Gose, 1971), the two characteristics in which we're interested are accuracy and sensitivity.
As regards the first property, the Receiving Operating Curve (ROC) is widely used to evaluate how well the fault is detected (Fawcett, 2006). Fig. 6a shows a ROC curve of $I2$, for the spring cracking fault mode, at a constant severity: the bender on the left is the curve, the higher is accuracy; the red line represents a 50% accuracy feature. Particularly, at a constant severity detection threshold (i.e. 30%), the Area Under the ROC Curve (AUC) provides a measure of feature's accuracy (Bradley, 1997).
Complementary to the previous performance metric that compares the features at the same severity, the success function (Fig. 6b) assesses the Probability Of Detection (POD) over the entire severity range (Vachtsevanos et al., 2007). The POD threshold has been defined to 95% in order to obtain acceptable errors margins (Mornacchi, Vachtsevanos, & Jacazio, 2015), therefore, at this level correspond the severity at detection that has been selected as sensitivity measure.

3.2.5. Accuracy-Sensitivity Plane

The end result of the feature selection process is the accuracy-sensitivity plane shown in Fig. 7, in which the performance metrics are displayed on the axes, while the correlation coefficient is identified by the color map and data's radius is proportional to the SNR.
In such a plane the best features are the bigger circles closest to the $(0, 1)$ point; moreover, looking at Fig. 7 is clear that the correlation information is congruent to the performance metrics but at the same time is inadequate as the only ranking criteria.
Against this background, the most convenient in-flight features are $I3$ for the spring cracking and $I6$ for the seals wear. As regards the on-ground features, $G3$ exhibits the best performances in both faults modes but it showed an opposite behaviour: it increases when spring crack occurs and conversely decreases as leakages consequence. Moreover, concurrent degradations haven't been studied so that $G3$ has been preferred for both faults modes.

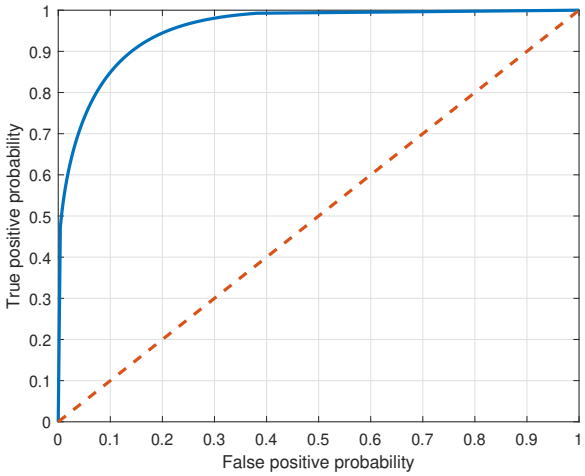

(a) ROC curve at 30% severity.

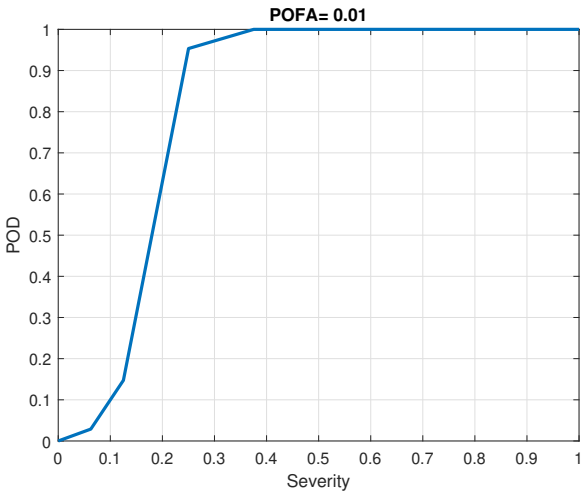

(b) Success function.

Figure 6. Spring cracking I2 performances.

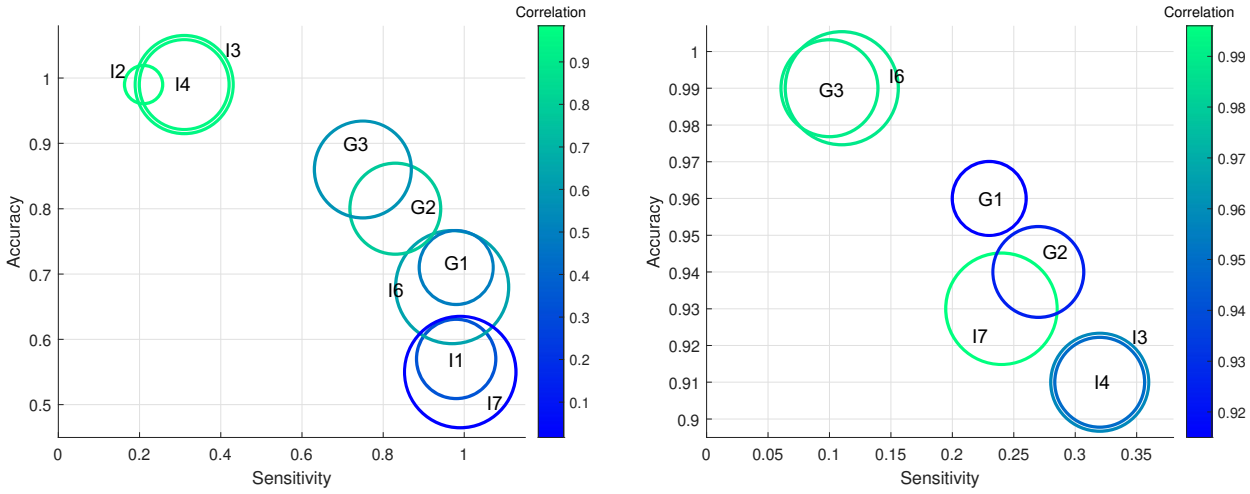

(a) Spring cracking.

(b) Seal wear: I1 and I2 out of range.

Figure 7. Accuracy-Sensitivity plane results.

4. PHM FRAMEWORK

The implemented PHM framework is based on an enhanced particle filter which is thorough described by authors in (De Martin, Jacazio, & Sorli, 2017).
The first requirement of the prognostics algorithm to estimates the marginal distribution:

$$p\left(\mathbf{x}_t|\mathbf{y}_{1:t}\right) \tag{6}$$

Where $\mathbf{x}_t$ is the hidden state (i.e. fault state) and $\mathbf{y}_t$ is the noisy measurements at time t, while:

$$\begin{cases} \mathbf{x}_{0:t} = \{\mathbf{x}_0, \ldots, \mathbf{x}_t\} \\ \mathbf{y}_{1:t} = \{\mathbf{y}_1, \ldots, \mathbf{y}_t\} \end{cases} \tag{7}$$

In the general case of a dynamical non-linear system affected by non-Gaussian noise, the state-space approach leads to the following recursion (Doucet, Arnaud de Freitas, Nando Gordon, 2001):

$$p\left(\mathbf{x}_t|\mathbf{y}_{1:t-1}\right) = \int p\left(\mathbf{x}_t|\mathbf{x}_{t-1}\right)\, p\left(\mathbf{x}_{t-1}|\mathbf{y}_{1:t-1}\right)\, d\mathbf{x}_{t-1} \tag{8}$$

That recursion needs also the knowledge of the previous state $p\left(\mathbf{x}_{t-1}|\mathbf{y}_{1:t-1}\right)$. Eq. (8), typically, cannot be computed analytically so many numerical methods have been developed (Arulampalam, Maskell, Gordon, & Clapp, 2002). Among all the possible integration methods we're interested in the particle filter which have found a large application in prognostics (Orchard, 2006).
With this name is indicated a subset of Monte Carlo methods based on numerical sampling. N samples *i.i.d.*

$$\{\mathbf{x}_{0:t}^{(i)},\ i = 1, \ldots,\ N\} \tag{9}$$

are linked to a related importance weight $\{\mathbf{x}_t^{(i)},\ \widetilde{w}_t^{(i)}\}_{i=1}^N$ in order to approximate Eq. (8) with the following:

$$p\left(\mathbf{x}_t|\mathbf{y}_{1:t}\right) \simeq \widetilde{w}_{0:t}^{(i)}\, \delta\left(\mathbf{x}_{0:t} - \mathbf{x}_{0:t}^{(i)}\right)\, d\mathbf{x}_{0:t-1} \tag{10}$$

Where δ is the Dirac delta function.
A sampling importance resampling (SIR) algorithm permits to obtain the importance sampling distribution through the $\mathbf{y}_t$ conditional probability:

$$\widetilde{w}_t^{(i)} \propto \widetilde{w}_{t-1}^{(i)}\, p\left(\mathbf{y}_t|\mathbf{x}_t^{(i)}\right) \tag{11}$$

then to compute Eq. (8).
The resampling step is fundamental to overcame the degeneracy problem (Doucet, 1998), or rather, the weights becoming negligible just after few iterations increasing the algorithm's computational complexity (Doucet, Godsill, & Andrieu, 2000).
Besides the illustrated filtering step, that aims to compute the pdf of the actual state of the system, the prediction step allows to compute the pdf of the system's state at the next time. The iteration of the prediction step generates a long-term prediction, then the pdf at time $t + p$ is estimated: $p\left(\mathbf{x}_{t+p}|\mathbf{y}_{1:t}\right)$ (Orchard & Vachtsevanos, 2009).
Finally, the long-term prediction is applied to estimate the pdf of the Remaining Useful Life (RUL) and the correlated risk of failure as illustrated in (Acuña & Orchard, 2018).

Table 3. Average RA and CRA.

	RA	CRA
Spring Cracking	84%	82%
Seals Wearing	93%	95%

4.1. Fault Detection

The adopted fault detection algorithm is purely data-driven and analogues to the first approach pursued in (De Martin, Jacazio, & Vachtsevanos, 2017).
The baseline and the actual PMFs (as shown in Fig. 5a) are constantly compared, as the current feature distribution shifts the fault probability arises and as soon as the overall confidence reaches a threshold of 95% the fault is detected.
Fault detection performance have been already analysed in section 3.2.5 and as shown, Fig. 7 summarizes this information. By looking at the selected features: the severity at detection in-flight is equal to 21% for the spring crack and to 11% for the seals wear, in both fault cases the POD is equal to 95%.

4.2. Failure Prognosis

An example of the prognosis output, based on the enhanced particle filter explained in section 4, is shown in Fig. 9 obtained applying the algorithm to the case of the seals wearing.
In the lowest plot of Fig. 9 is clarified the relationship between the RUL pdf and the risk function. The Acuña's discrete time risk function is the cumulative distribution function of the Probability of Failure (PoF) (Acuña & Orchard, 2018):

$$\mathcal{R}_A\left(t_f = k|\mathbf{y}_{1:k_p}\right) = \mathcal{P}\left(t_f \leq k|\mathbf{y}_{1:k_p}\right) = \\ = \sum_{i=k_p+1}^{k} \mathcal{P}\left(t_f = i|\mathbf{y}_{1:k_p}\right) \quad (12)$$

Where t_f is the time of failure, while, k_p is the time when the prognostics algorithm is executed.
The performance prognostic algorithm have been investigated through some of the metrics proposed in (Saxena et al., 2008), specifically the four metrics scheme suggested in (Saxena, Celaya, Saha, Saha, & Goebel, 2010). The analysis $\alpha-\lambda$, depicted in Fig. 8 applied to the seals wearing case, shown that the algorithm performs within the desired error margin of $\alpha = 20\%$ at any time. Besides, relative accuracy (RA) and cumulative relative accuracy (CRA) information have been extracted from previous analysis; the overall results are reported in Table 3. The averages indicate that the selected features together with the PF-based prognostic routine, have reaped satisfying results, as regards accuracy and convergence properties in both fault modes.

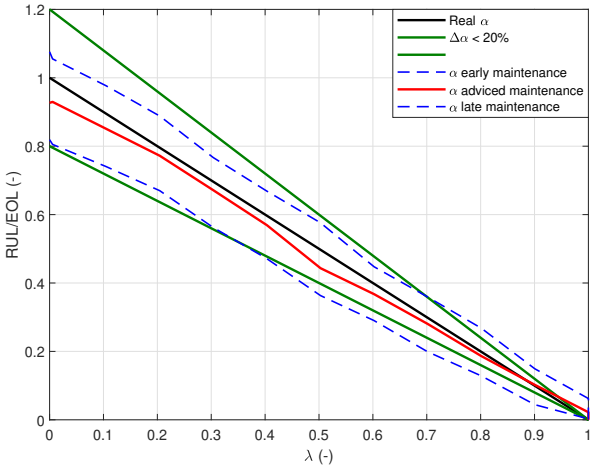

Figure 8. $\alpha - \lambda$ accuracy (seals wearing).

5. CONCLUSION AND FUTURE WORKS

The present research has been focused on a uncharted field of prognostics application, or rather, it has shown the feasibility of a PHM system for helicopters' MRA and TRA under the hypothesis of SCAS' fault modes independence. Moreover, the aim has been obtained without the need of additional sensors, so that the prognostics algorithm is applicable for operating helicopters' flight control actuators.
A rigorous approach has led to an accurate description of fault models and many simulations has been carried out, in many different configuration, so as to achieve a statistically significant data set.
The in-depth feature selection has demonstrated that the correlation coefficient is inadequate as the only ranking criteria, whereas a reliable feature selection metric, based on features actual detection properties, has been defined which has been outlined in the accuracy-sensitivity plane (i.e. a new way to visualize feature selection results). The selected features proved to detect the fault and predict the RUL with satisfying accuracy, as show in the $\alpha - \lambda$ plane.
Further studies will be conducted in order to include more faults modes in the PHM algorithm, regarding both SCAS' actuators and EHSVs. Although, in a general lack of literature references, the paper outlines an interesting applicability field for PHM systems that could be able to bring large benefits to the helicopters' reliability.

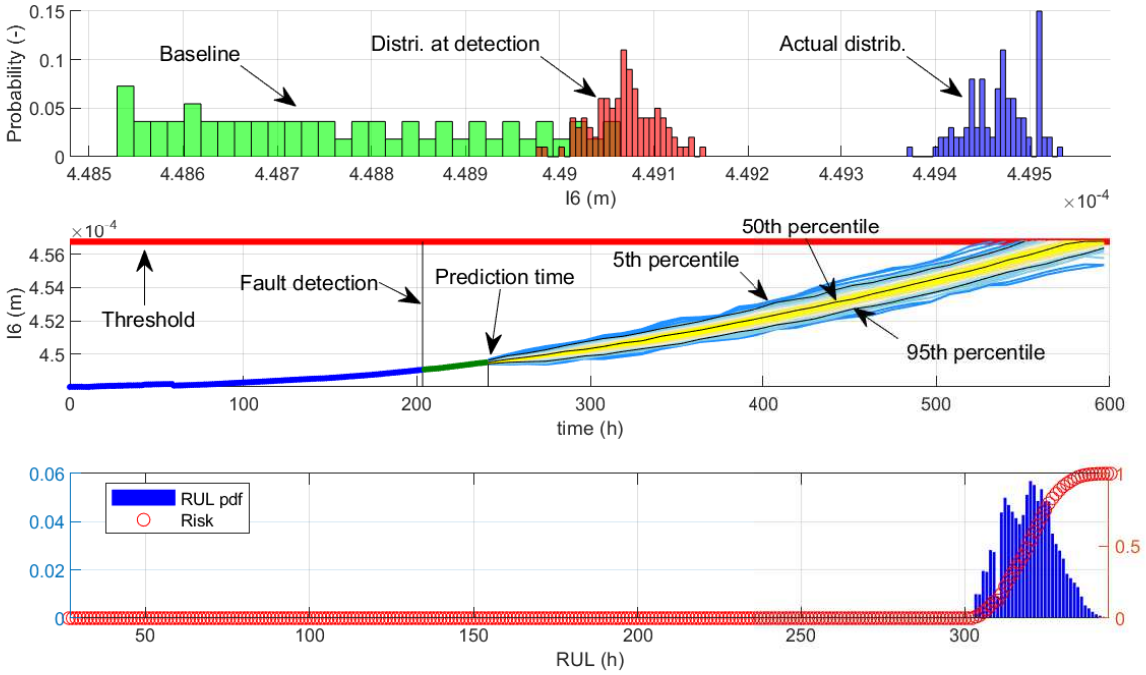

Figure 9. Prognostics results (seals wearing).

NOMENCLATURE

$\mathcal{R}_A$	Acuña's risk function
D_{KL}	Kulloback-Leibler divergence
$i.i.d.$	Indipendent and Identical Distributed
L_a	Work of friction forces
$p(\cdot)$	Probability density function
$p(\cdot\|\cdot)$	Conditional probability
Q_l	Internal flow rate leakages
$\mathbb{E}[\cdot]$	Expected value
μ_x	Mean value of x
ρ_{DF}	Pearson's correlation between D and F
σ_x	Standard deviation of x
AUC	Area Under the (ROC) Curve
CRA	Cumulative Relative Accuracy
$EHSV$	Electro Hydraulic Servo Valve
FFT	Fast Fourier Transform
FRF	Frequency Response Function
MRA	Main Rotor Actuator
PDF	Probability Density Function
PHM	Prognostics and Health Management
PMF	Probability Mass Function
POD	Probability Of Detection
$POFA$	Probability Of False Alarm
RA	Relative Accuracy
RMS	Root Mean Square
ROC	Receiving Operating Curve
$SCAS$	Stability and Command Augmentation System
SIR	Sampling Importance Resampling
SNR	Signal to Noise Ratio
TRA	Tail Rotor Actuator

REFERENCES

Acuña, D. E., & Orchard, M. E. (2018). A theoretically rigorous approach to failure prognosis. In *Proceedings of the annual conference of the prognostics and health management society, phm.*

Adams, S., Meekins, R., Beling, P. A., Farinholt, K., Brown, N., Polter, S., & Dong, Q. (2017). A comparison of feature selection and feature extraction techniques for condition monitoring of a hydraulic actuator. In *Proceedings of the annual conference of the prognostics and health management society, phm.*

Archard, J. F. (1953). Contact and rubbing of flat surfaces. *Journal of Applied Physics*. doi: 10.1063/1.1721448

Arulampalam, M. S., Maskell, S., Gordon, N., & Clapp, T. (2002). A tutorial on particle filters for online nonlinear/non-Gaussian Bayesian tracking. *IEEE Transactions on Signal Processing*. doi: 10.1109/78.978374

Autin, S., Socheleau, J., Dellacasa, A., De Martin, A., Jacazio, G., & Vachtsevanos, G. (2018). Feasibility study of a PHM system for electro-hydraulic servoactuators for primary flight controls. In *Proceedings of the annual conference of the prognostics and health management society, phm.*

Bertolino, A. C., Gentile, R., Jacazio, G., Marino, F., & Sorli, M. (2018). EHSA primary flight controls seals wear

degradation model. In *Asme international mechanical engineering congress and exposition, proceedings (imece)*. doi: 10.1115/IMECE2018-87080

Blum, A. L., & Langley, P. (1997). Selection of relevant features and examples in machine learning. *Artificial Intelligence*. doi: 10.1016/s0004-3702(97)00063-5

Bradley, A. P. (1997). The use of the area under the ROC curve in the evaluation of machine learning algorithms. *Pattern Recognition*. doi: 10.1016/S0031-3203(96)00142-2

Dash, M., & Liu, H. (1997). Feature selection for classification. *Intelligent Data Analysis*. doi: 10.3233/IDA-1997-1302

De Martin, A., Dellacasa, A., Jacazio, G., & Sorli, M. (2018). High-fidelity model of electro-hydraulic actuators for primary flight control systems. In *Bath/asme 2018 symposium on fluid power and motion control, fpmc 2018*. doi: 10.1115/FPMC2018-8917

De Martin, A., Jacazio, G., & Sorli, M. (2017). Enhanced Particle Filter framework for improved prognosis of Electro-Mechanical flight controls Actuators. *3rd European Conference of the Prognostic and Health Management Society*, 1–10.

De Martin, A., Jacazio, G., & Vachtsevanos, G. J. (2017). Windings fault detection and prognosis in electromechanical flight control actuators operating in active-active configuration. *International Journal of Prognostics and Health Management*.

Doucet, A. (1998). On Sequential Simulation-Based Methods for Bayesian Filtering. *Signal Processing*. doi: 10.1.1.361.4361

Doucet, A., Godsill, S., & Andrieu, C. (2000). On sequential Monte Carlo sampling methods for Bayesian filtering. *Statistics and Computing*. doi: 10.1023/A:1008935410038

Doucet, Arnaud de Freitas, Nando Gordon, N. (2001). *Sequential Monte Carlo Methods in Practice*. doi: 10.1007/978-1-4757-3437-9

Elattar, H. M., Elminir, H. K., & Riad, A. M. (2016). Prognostics: a literature review. *Complex & Intelligent Systems*. doi: 10.1007/s40747-016-0019-3

Fawcett, T. (2006). An introduction to ROC analysis. *Pattern Recognition Letters*. doi: 10.1016/j.patrec.2005.10.010

Grosso, L. A., De Martin, A., Jacazio, G., & Sorli, M. (2018). Development of data-driven PHM solutions for robot hemming in automotive production lines. , 1–13.

Kullback, S., & Leibler, R. A. (1951). On Information and Sufficiency. *The Annals of Mathematical Statistics*. doi: 10.1214/aoms/1177729694

Mackay, D. J. C. (2005). Information Theory, Inference, and Neural Networks. , 628.

Macky, D. W., & Roussas, G. C. (1999). A Course in Mathematical Statistics. *The American Statistician*. doi: 10.2307/2685661

Mornacchi, A., Vachtsevanos, G., & Jacazio, G. (2015). Prognostics and health management of an electro-hydraulic servo actuator. In *Proceedings of the annual conference of the prognostics and health management society, phm.*

Mucciardi, A. N., & Gose, E. E. (1971). A Comparison of Seven Techniques for Choosing Subsets of Pattern Recognition Properties. *IEEE Transactions on Computers*, *C-20*(9), 1023–1031. doi: 10.1109/T-C.1971.223398

Nesci, A., De Martin, A., Jacazio, G., & Sorli, M. (2020). Detection and Prognosis of Propagating Faults in Flight Control Actuators for Helicopters. *Aerospace*. doi: 10.3390/aerospace7030020

Orchard, M. E. (2006). A Particle Filtering-based Framework for On-line Fault Diagnosis and Failure Prognosis. *School of Electrical and Computer Engineering, Georgia Institute of Technology*.

Orchard, M. E., & Vachtsevanos, G. J. (2009). A particle-filtering approach for on-line fault diagnosis and failure prognosis. *Transactions of the Institute of Measurement and Control*. doi: 10.1177/0142331208092026

Paris, P., & Erdogan, F. (1963). A critical analysis of crack propagation laws. *Journal of Fluids Engineering, Transactions of the ASME*. doi: 10.1115/1.3656900

Samuel, P. D., & Pines, D. J. (2005). A review of vibration-based techniques for helicopter transmission diagnostics. *Journal of Sound and Vibration*. doi: 10.1016/j.jsv.2004.02.058

Saxena, A., Celaya, J., Balaban, E., Goebel, K., Saha, B., Saha, S., & Schwabacher, M. (2008). Metrics for evaluating performance of prognostic techniques. In *2008 international conference on prognostics and health management, phm 2008.* doi: 10.1109/PHM.2008.4711436

Saxena, A., Celaya, J., Saha, B., Saha, S., & Goebel, K. (2010). Metrics for offline evaluation of prognostic performance. *International Journal of Prognostics and Health Management*.

Vachtsevanos, G., Lewis, F., Roemer, M., Hess, A., & Wu, B. (2007). *Intelligent Fault Diagnosis and Prognosis for Engineering Systems*. doi: 10.1002/9780470117842